Dynamic Light Scattering Study on Particle Diffusion in Slide-Ring Gels: Enhanced Fluctuation of Sliding Networks

Yusuke Yasuda, Hiroki Matsunobu, Tetsuharu Narita, Hideaki Yokoyama, Koichi Mayumi, Kohzo Ito

Dynamic Light Scattering Study on Particle Diffusion in Slide-Ring Gels: Enhanced Fluctuation of Sliding Networks

Yusuke Yasuda[1], Hiroki Matsunobu[1], Tetsuharu Narita[2,3], Hideaki Yokoyama[1], Koichi Mayumi[1,4,*], Kohzo Ito[1,*]

[1] Material Innovation Research Center (MIRC) and Department of Advanced Materials Science, Graduate School of Frontier Sciences, The University of Tokyo, 5-1-5 Kashiwanoha, Kashiwa, Chiba 277-8561, Japan.

[2] Laboratoire Sciences et Ingénierie de la Matière Molle, ESPCI Paris, PSL University, Sorbonne Université, CNRS, 10 rue Vauquelin, 75231, Paris, Cedex 05, France.

[3] Global Station for Soft Matter, Global Institution for Collaborative Research and Education, Hokkaido University, Sapporo, Japan.

[4] AIST-UTokyo Advanced Operando-Measurement Technology Open Innovation Laboratory (OPERANDO-OIL), National Institute of Advanced Industrial Science and Technology (AIST), 5-1-5 Kashiwanoha, Kashiwa, Chiba 277-8561, Japan.

*Correspondence: koichi.mayumi@edu.k.u-tokyo.ac.jp (K.M.); kohzo@edu.k.u-tokyo.ac.jp (K.I.); Tel.: +81-4-7136-3768 (K.M.); +81-4-7136-3756 (K.I.)

Abstract

In slide-ring (SR) gels, polymer chains are cross-linked by rings and can slide through the cross-linking points. The high chain mobility in SR gels is responsible for their unique physical properties such as softness, high deformability, and crack resistance. In this study, the dynamics of the polymer network in SR gels was investigated by the microrheological technique. The diffusion coefficients of the silica nanoparticles in SR gels with different cross-linking densities were measured by dynamic light scattering (DLS). It was found that the diffusion coefficient of the probe particles in the SR gels does not decrease monotonically with increasing cross-linking density even though their mesh sizes are close to the particle size. This suggests that the slidability of the cross-linking points enhances fluctuation of the polymer networks in the SR gels.

Keywords

Dynamic Light Scattering; Slide-Ring Gel; Micro-Rheology, Polymer Gel; Probe Diffusion

1. Introduction

Slide-ring (SR) gels are polymer networks which are cross-linked by ring molecules[1–3]. In 2001, Okumura and Ito fabricated SR gels by cross-linking the ring molecules of polyrotaxane (PR), a necklace-like supramolecule composed of α-cyclodextrin (CD) and polyethylene glycol (PEG)[4]. In SR gels, polymer chains can slide through the movable cross-linking points consisting of two connected rings, and are expected to have higher chain mobility as compared with conventional polymer gels cross-linked by covalent bonds. In practice, SR gels show unique physical properties related to the high mobility of polymer networks, such as low Young's moduli (softness)[5,6], high deformability[5,7], crack resistance[6,8], and pressure-induced solvent permeation[9].

In order to reveal the molecular origin of the macroscopic properties of SR gels, their static polymer network structure under deformation has been studied by small-angle X-ray scattering (SAXS)[10] and neutron scattering (SANS)[11–13]. In the case of conventional fixed-crosslinking (FC) gels with covalent cross-links, the inhomogeneity of the network structure increases with strain, and the enhanced

inhomogeneity causes stress concentration on the short network strands and brittle fracture of the gels[11]. Conversely, for SR gels, the polymer network structure in stretched SR gels is more homogeneous and isotropic owing to the slidability of the cross-linking points[10,11], which leads to the high deformability and toughness of SR gels. However, the dynamic fluctuation of the polymer network in SR gels has not been fully understood yet.

The dynamics of the polymer networks in gels has been investigated using dynamic light scattering (DLS)[14,15]. The DLS measurements of polymer gels detect a cooperative diffusion mode corresponding to the thermal fluctuation of concentration blobs in the polymer networks. In the case of the SR gels, cooperative diffusion modes have also been observed by DLS[16,17]. However, as the spatial range for DLS (around 100 nm order) is much larger than the nm-scale of the ring molecules and the network size in SR gels, it is difficult to correlate the cooperative modes probed by DLS with the sliding motion in SR gels.

In this study, we investigated the polymer dynamics of SR gels by means of a microrheological method based on DLS. Silica nanoparticles were introduced into SR gels and fixed cross-link (FC) gels with covalent cross-links, and the diffusion coefficients of the nanoparticles in SR and FC gels were measured by DLS. The

dynamics of the polymer networks influences the diffusion dynamics of the dispersed nanoparticles with almost the same size as the meshes of the gels. For conventional FC gels, the diffusion of the nanoparticles is suppressed with increasing cross-linking density of the gels (decreasing mesh size)[18]. From our DLS experiments, we found that the diffusion coefficients of silica nanoparticles in SR gels does not decrease monotonically with cross-linking density, which indicates an enhanced fluctuation of the cross-linking points by the sliding dynamics.

2. Materials and Methods

2.1 Sample Preparation

The SR gels were prepared by cross-linking hydroxypropylated polyrotaxane, HAPR (Advanced Softmaterials Inc.) consisting of PEG (M_w = 3.5×10^4 g/mol), and hydroxypropylated α-cyclodextrin (CD) (hydroxypropylation ratio = 50 %). The ring coverage ratio on PEG was 25%. HAPR was dissolved in NaOH aqueous solution. Silica nanoparticles aqueous solution (Sigma-Aldrich LUDOX® SM-30) was filtered with a hydrophilic PTFE syringe filter (Φ= 0.45 μm) , and then was added into the polyrotaxane solution with final concentrations of 0 wt%, 1 wt%, 2wt% and 3 wt%. Finally, divinyl sulfone was added as a cross-linker to cross-link hydroxyl groups of

CDs. The cross-linker concentration was varied to control the cross-linking density of the gels. The HAPR and NaOH concentrations in the gels were 10 wt% and 0.01 M, respectively. The pre-gel solutions were injected into to a 1-mm-thick mold for tensile and SAXS measurements. For DLS measurements, the pre-gel solutions were filtered with a hydrophilic PTFE syringe filter (Φ= 0.45 μm), and then were poured in test tubes (diameter: 10 mm). The molds and test tubes were placed at room temperature for over 100 hours for gelation. For comparison, we prepared fixed cross-link (FC) gels from pullulan (Hayashibara Inc., M_w = 9.9×10^4 g/mol) in the same way as the SR gels. The cross-linker concentration for the pullulan gels was tuned for their Young's moduli close to those of the SR gels.

For SAXS measurements, silica nanoparticle solutions were also prepared. The silica nanoparticles were dispersed in NaOH 0.01 M aqueous solution with silica concentrations of 1 wt% and 3 wt%.

2.2 Uniaxial Tensile Test

Uni-axial tensile tests on the SR and FC gels with/without silica nanoparticles were carried out. We used a Shimadzu EZ-S universal tester with a 5 N load cell. The size of sample specimens was 15 mm×3 mm×1 mm, and the samples were stretched at a

speed of 5%/s at room temperature until it fractured.

2.3 Small-Angle X-ray Scattering

Small-angle X-ray scattering (SAXS) measurements were carried out at BL6A at Photon Factory, High Energy Accelerator Research Organization, KEK (Ibaraki, Japan). The wavelength λ of the incident X-ray beam was 1.5 Å and the beam size was 0.5 mm (vertical)×0.5 mm (horizontal). The sample-to-detector distance was 2.6 m, and the 2D detector was PILATUS3 1M (DECTRIS). The exposure time for each measurement was 30 sec. The scattering angle θ was calibrated by the diffraction pattern of chicken tendon collagen. The obtained SAXS patterns were converted into 1D profiles, the scattering intensity, *I*, vs amplitude of scattering vector, *Q*, by circular averaging. The definition of *Q* is given as below:

$$Q = \frac{4\pi}{\lambda} \sin\left(\frac{\theta}{2}\right) \quad (1)$$

2.4 Dynamic Light Scattering

Dynamic light scattering (DLS) experiments were conducted with a DLS/SLS-5000 compact goniometer (ALV, Langen, Germany). The scattering angle θ

was changed from 30° to 150° in 30° steps. A He−Ne laser with 22 mW (wavelength 632.8 nm) was used as the incident beam. In order to circumvent the nonergodicity of the gels, the sample test tube was moved up and down vertically during the measurements. The time-averaged correlation functions of the scattered light intensity, $g^{(2)}(t)$, were measured at 25 °C for 1800 s and converted to the normalized correlation functions of the scattered field fluctuation $g^{(1)}(t)$.

3. Results and Discussion

3.1 Uniaxial Tensile Test

In order to evaluate the mesh size of the gels, uni-axial tensile tests were performed on SR and FC gels. The stress-strain curves of SR and FC gels without silica nanoparticles are shown in Figure 1. As mentioned in our previous work, SR gels show J-shaped curves, while the stress-strain curves of FC gels are S-shaped[5]. From the initial slopes (from 0% up to 20% strain) of the stress-strain curves, the Young's moduli of the gels were evaluated (Table 1). The SR and FC gels with high, middle, and low Young's moduli were named SR/FC_high, SR/FC_mid, and SR/FC_low, respectively. For FC gels, the Young's moduli can be converted to mesh sizes of the gels based on the rubber elasticity theory. From the affine network theory[19], Young's modulus E can be

expressed as a function of the number density of network strand between cross-links v, in the following manner:

$$E = 3\nu k_{\mathrm{B}}T \tag{2}$$

where k_{B} is Boltzmann constant, and T is absolute temperature. The number density of strands v is related to the mesh size ξ as follows:

$$\xi \approx \nu^{-\frac{1}{3}} = \left(\frac{3k_BT}{E}\right)^{\frac{1}{3}} \tag{3}$$

From Eq. (3) and the Young's moduli given in Table 1, the mesh sizes ξ of FC_low, FC_mid, and FC_high were estimated as 17, 12, and 9.5 nm, respectively. In the case of SR gels, the affine network model is not applicable because the cross-linking points in SR gels have large thermal fluctuation due to the sliding motion. In our previous work, we have demonstrated that the Young's modulus of SR gels is smaller than the affine network model prediction, and that the sliding motion of the cross-linking points reduces the Young's modulus[20,21]. As shown in Table 1, the SR gels show almost the same Young's moduli as the FC gels, even though the cross-linker concentrations in feed for the SR gels are higher than those for the FC gels. This means that the mesh sizes of the SR gels are smaller than the calculated values for the FC gels.

Uni-axial tensile tests for SR and FC gels with silica nanoparticles were also conducted. Figure 2 shows the silica concentration dependence of the Young's moduli for SR and FC gels with different cross-linker concentrations. For all the cross-linker concentrations, the Young's moduli of the silica-containing gels slightly increase with silica concentration. The filler concentration dependence of Young's modulus for filler-filled elastomers without interaction between polymer matrix and fillers can be described by Guth-Gold equation[22,23]:

$$E^*(c) = E(1 + 2.5\phi + 14.1\phi^2) \quad (4)$$

where E^* is the Young's modulus of a filler-filled elastomer, and E is the Young's modulus of the elastomer without filler, and ϕ is the volume fraction of the filler. As shown in Figure 2, the measured Young's moduli of the gels containing the silica particles are almost the same as, or slightly higher than the Guth−Gold prediction. Since the difference from the Guth-Gold theory is small compared with in the case of the nanocomposite gels in which polymer chains are strongly absorbed on the silica particles[23], the interaction between the silica particles and polymer networks of SR and FC gels is weak. Also, the SR and FC gels show similar silica concentration dependence of the Young's moduli, which indicates the weak interaction between the SR gels and particles is almost the same as that between the FC gels and particles.

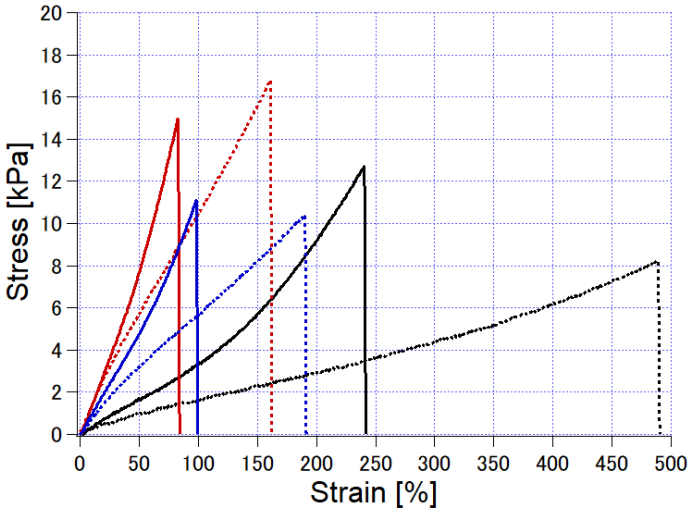

Figure 1. Stress-strain curves of SR and FC gels without silica nanoparticles. The cross-linker concentrations for FC gels were 0.3 wt% (red dotted line), 0.2 wt% (blue dotted line), and 0.1 wt% (black dotted line), while those for SR gels were 1.5 wt% (red solid line), 1.0 wt % (blue solid line), and 0.6 wt % (black solid line).

Table 1. Sample names, cross-linker concentrations, and Young's moduli for FC and SR gels without the silica nanoparticles.

Sample name	**FC_low**	**FC_mid**	**FC_high**	**SR_low**	**SR_mid**	**SR_high**
Cross-linker concentration [wt%]	0.1	0.2	0.3	0.6	1.0	1.5
Young's modulus *E* [kPa]	2.3	7.1	13.3	3.4	9.5	14.7

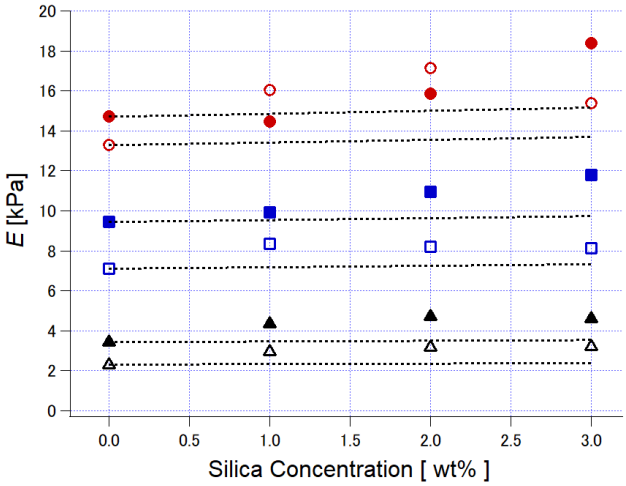

Figure 2. Silica concentration dependence of Young's modulus for FC_high (red open circle), SR_high (red filled circle), FC_mid (blue open square), SR_mid (blue filled square), FC_low (black open triangle), and SR_low (black filled triangle). The dotted black lines are the theoretical lines of Guth-Gold equation (Eq. (4).).

3.2 Small-Angle X-ray Scattering

To estimate the sizes of silica nanoparticles and their distribution in the gels, we carried out small-angle X-ray scattering (SAXS) measurements on the silica nanoparticle solutions and nanoparticle-dispersed SR/FC gels. Figures 3 (a) and (b) show the scattering profiles, scattering intensity, I, vs amplitude of scattering vector, Q, for the silica solutions and silica-containing SR/FC_low gels with silica concentrations

of 1 wt% and 3 wt%, respectively. For all the samples, the scattering intensities in the middle Q range decay as Q^{-4} corresponding to the form factor of spheres. The scattering profiles of the silica nanoparticle solutions were fitted with the form factor for spheres with size distribution[24]:

$$I(Q) = \int_0^\infty \frac{9}{\sqrt{2\pi\sigma^2}} \exp\left(-\frac{(r-R)^2}{2\sigma^2}\right) \frac{(\sin Qr - Qr\cos Qr)^2}{(Qr)^6} \mathrm{d}r \qquad (5)$$

where Q is the amplitude of the scattering vector, R is the radius of the particle, and σ is the standard deviation of the radius. From the fitting, the radius of the silica particles was estimated as 6.6 ± 1.4 nm (silica = 1 wt %) and 6.8 ± 1.5 nm (silica = 3 wt%). The obtained particle size is on the same order of magnitude as the mesh sizes of FC gels estimated by the uniaxial tensile tests. Additionally, the scattering profiles of SR and FC gels with silica nanoparticles are similar to those of the silica solutions in the low Q range, which suggests that the silica nanoparticles are well dispersed in all the gels, and that the particle dispersion is almost the same for the SR and FC gels. The difference of the scattering profiles in the high Q range between the silica solutions and gels with silica particles corresponds to the scattering from the polymers (see the supporting information).

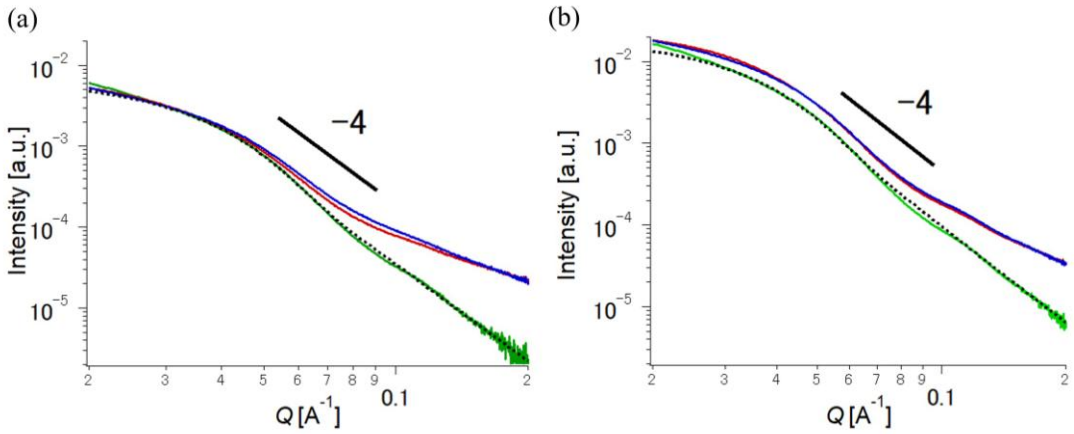

Figure 3. Small-angle X-ray scattering profiles of FC_low gels (blue line), SR_low gels (red line) and silica suspension (green line) with (a) 1 wt % and (b) 3 wt % silica concentrations. The dotted lines are the fitting results by Eq. (5).

3.3 Dynamic Light Scattering

Next, we performed DLS measurements of the SR and FC gels with/without silica nanoparticles. Figures 4 (a) and (b) show the normalized autocorrelation functions $g^{(1)}(t)$ at a scattering angle of 90° for FC_low and SR_low gels with different silica concentrations (0 wt%, 1 wt%, 2 wt%, and 3 wt%). Both FC and SR gels without silica particles show a typical dynamic behavior of chemical gels: they exhibit a relaxation mode at about 0.05 ms, corresponding to the cooperative diffusion mode of the polymer

networks[15,16], followed by a plateau ascribed to the static heterogeneity of concentrations. For the gels with silica nanoparticles, another slow mode appears at about 10 ms, and the relaxation amplitude increases with the silica concentration. This mode can be attributed to the dynamics of the silica nanoparticle in the gels[18].

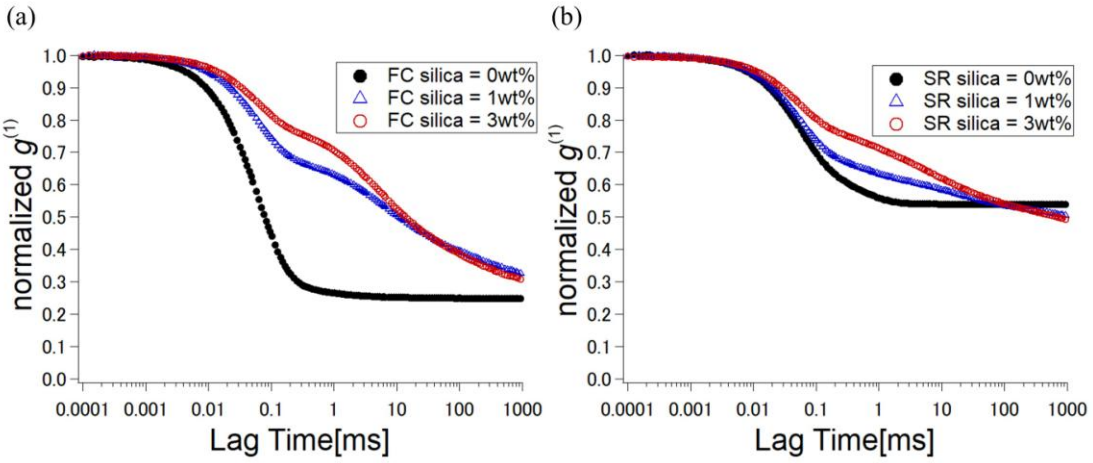

Figure 4. Normalized autocorrelation function $g^{(1)}(t)$ at scattering angle 90° for (a) FC_low gel and (b) SR_low gel with 0% (black filled circle), 1 wt% (blue open triangle), and 3 wt% (red open circle) silica particles.

To study the effect of the cross-linker concentration on the dynamics of the silica nanoparticles, the probe particle dynamics in the silica-containing FC and SR gels with different cross-linker concentrations were measured. The obtained normalized correlation functions $g^{(1)}(t)$ for the FC and SR gels with 1wt% silica concentration are

shown in Figures 5(a) and (b). For quantitative analysis, we fitted the relaxation curves $g^{(1)}(t)$ using the following equation :

$$g^{(1)}(t) = A_{\mathrm{gel}} \exp\left(-\left(\frac{t}{\tau_{\mathrm{gel}}}\right)\right) + A_{\mathrm{silica}} \exp\left(-\left(\frac{t}{\tau_{\mathrm{silica}}}\right)^{\beta_{\mathrm{silica}}}\right) + 1 - A_{\mathrm{gel}} - A_{\mathrm{silica}} \qquad (6)$$

where A_i and τ_i are the relaxation amplitude and relaxation time of the gel/silica mode (i = gel or silica) , respectively. β_{silica} is a parameter to express the distribution of the relaxation time for the silica dynamics. The fitting results are summarized in Table 2. The plateau value, $1 - A_{\mathrm{gel}} - A_{\mathrm{silica}}$, increases with the increase in the cross-linker concentration, corresponding to the increased spatial heterogeneity of the network.

In order to further characterize the dynamics of the silica particles in these gels, Q dependence of the relaxation time for the silica particle was investigated. Q is given by the following equation:

$$Q = \frac{4\pi n}{\lambda} \sin\left(\frac{\theta}{2}\right) \qquad (7)$$

where λ is the wavelength of the incident laser, n is the refractive index of the solvent (n =1.33 for water), and θ is the scattering angle. The relaxation time of the silica particle has a distribution represented by β_{silica}, and the average relaxation time $\langle\tau_{\mathrm{silica}}\rangle$was calculated from the following equation[25, 26]:

$$\langle\tau_{\mathrm{silica}}\rangle = \frac{\Gamma\left(\frac{1}{\beta_{\mathrm{silica}}}\right)}{\beta_{\mathrm{silica}}} \tau_{\mathrm{silica}} \qquad (8)$$

Figure 6 shows the scattering vector Q dependence of the obtained $\langle\tau_{\mathrm{silica}}\rangle$ for SR_low

and FC_low gels with silica concentration of 1 wt%. The average relaxation time $\langle\tau_{\mathrm{silica}}\rangle$ of the gels decays as Q^{-2}, which means that the dynamics of the silica particles are diffusive. The diffusion coefficients of the silica nanoparticles in the gels are given as:

$$D_{\mathrm{silica}} = \frac{1}{Q^2\langle\tau_{\mathrm{silica}}\rangle} \tag{9}$$

From Eq. (9) and $\langle\tau_{\mathrm{silica}}\rangle$, the diffusion coefficients of the silica nanoparticles in the FC and SR gels D_{silica} were estimated and plotted against the Young's moduli of the gels without silica (shown in Figures 7(a) and (b)). The diffusion coefficients of the silica nanoparticles in the gels were 0.5 to 8.5×10^{-10} cm^2/s, which is much lower than that of the silica particle in 0.01M NaOH aquaeous solution at 25℃, 2.0×10^{-7} cm^2/s. This suggests that the diffusion of the silica particle is suppressed in the gels. As shown in Figure 7 (a), with decreasing mesh size of the FC gels from 17 nm to 9.5 nm, D_{silica} decreases significantly and approaches to zero, which is consistent with a previous work on particle diffusion in polyacrylamide gels[18]. For FC_high gel, the mesh size estimated from the Young's modulus is 9.5 nm, which is close to the radius of the silica nanoparticle, 6.6 nm. Conversely, the diffusion coefficient of the silica nanoparticles in the SR gels does not decrease monotonically with increasing Young's modulus, but shows a weaker dependence on the Young's modulus compared to that for FC gels. It is

worthwhile to note that D_{silica} for SR_high is much larger than that for FC_high, although the former has a smaller mesh size than the latter. The large values of D_{silica} and the weak dependence of D_{silica} on the Young's modulus (mesh size) are probably because of the enhanced fluctuation of the polymer network in the SR gels.

For FC gels, the diffusion coefficient of the silica nanoparticles is dominated by the mesh size of the fixed cross-linking network structure. When the mesh size is close to the particle size, the diffusion of the particles is significantly retarded by the friction between the polymer network and particles (Figure 8 (a)). However, for SR gels, the cross-linking points slide on the polymer chains and the network structure fluctuates. Thus, even if the particle size is close to or smaller than the average mesh size, the nanoparticles are not trapped, but diffuse in the slide-ring networks (Figure 8 (b)). This is the first study to detect the nano-scale fluctuation of cross-links originating from the sliding motion in SR gels. The high mobility of the polymer network in SR gels is the molecular origin of their softness (low Young's modulus). For conventional polymer networks, the phantom network model takes into account the thermal fluctuation of cross-linking points while the affine network model assumes that the cross-linking points are fixed in space[27]. The Young's modulus calculated by the phantom network model is half as large as that estimated from the affine network model, which means

that the thermal fluctuation of cross-links reduces the Young's modulus. The quantitative relation between the cross-links' sliding mobility and the Young's modulus of SR gels will be studied in future work. In addition to the rheological properties, the fluctuation of the network structure in SR gels influences their permeation behaviors. The dynamic network fluctuation observed by the probe diffusion measurements is crucial to control the permeation properties of SR gels.

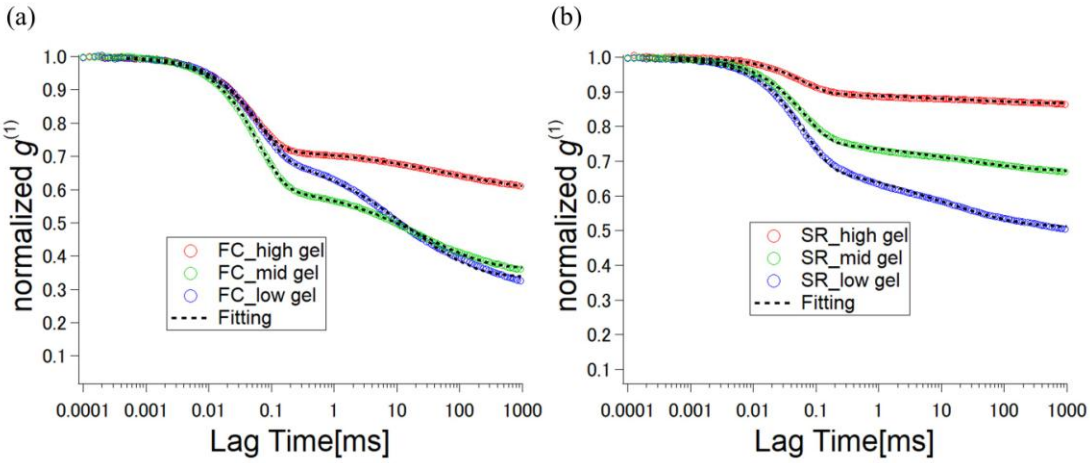

Figure 5. Normalized autocorrelation function $g^{(1)}$ (t) at 90 ° scattering angle for (a) FC and (b) SR gels with different cross-linker concentrations and silica concentration = 1wt%: FC/SR_high (red open circle), FC/SR_mid (blue open circle), and FC/SR_low (green open circle). The black dotted lines are the fitting results by Eq. (6).

Table 2. Fitting parameters for the DLS results of FC and SR gels with 1 wt% silica particle (scattering angle 90 °).

	A_{gel}	A_{silica}	τ_{gel} [ms]	τ_{silica} [ms]	β_{silica}
FC_low	0.27	0.40	0.065	16	0.41
FC_mid	0.38	0.26	0.062	29	0.43
FC_high	0.27	0.13	0.054	72	0.36
SR_low	0.29	0.20	0.066	10	0.35
SR_mid	0.23	0.10	0.064	16	0.30
SR_high	0.10	0.035	0.061	16	0.30

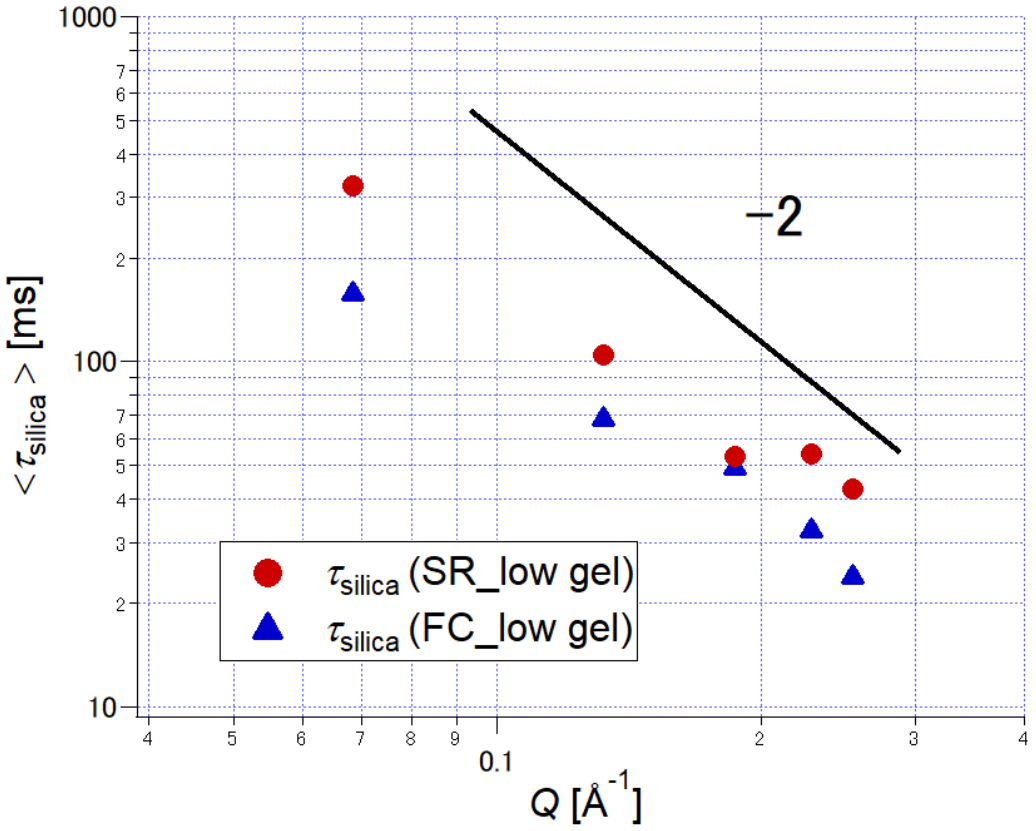

Figure 6. *Q* dependence of τ_{silica} for FC/SR_low gel with silica concentration = 1 wt%.

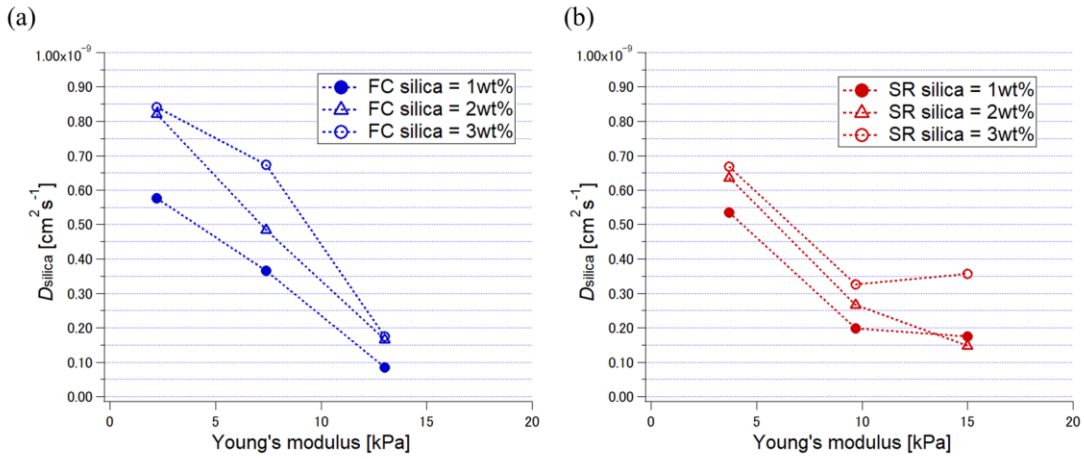

Figure 7. Plot of diffusion coefficients of silica nanoparticle in (a) FC and (b) SR gels versus the Young's moduli of the gels without silica nanoparticle.

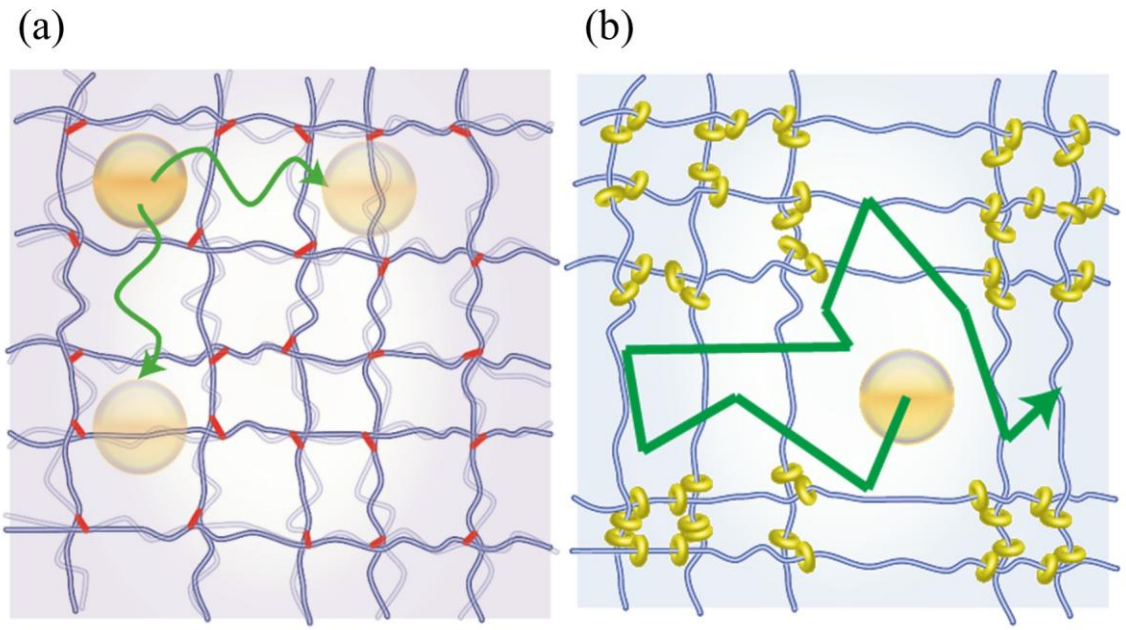

Figure 8. Schematic illustration showing the diffusion of a nanoparticle in (a) FC and (b) SR networks.

4. Conclusions

The diffusion of silica nanoparticles in SR and FC gels was studied to reveal the nanoscale sliding dynamics of the cross-links. The mesh sizes of the gels estimated from their Young's moduli are on the same order of magnitude as the silica particle size. From the SAXS experiments, it was found that the silica particles are well dispersed in both the gels. Subsequently, DLS measurements were performed to evaluate the

diffusion coefficients of the silica nanoparticles, D_{silica}, in the FC and SR gels. While D_{silica} in the FC gels decreases with increasing Young's modulus of the gels, the Young's modulus dependence of D_{silica} for the SR gels is weak. Especially for high cross-linking density (high Young's moduli), D_{silica} in the SR gels is larger than that in the FC gel. This result suggests that the SR gels have larger network fluctuation than the FC gels because of the sliding of the cross-links. This is the first experimental evidence of the nano-scale high mobility of polymer networks in SR gels, which is responsible for their macroscopic mechanical softness (low Young's modulus). Furthermore, the network dynamics of SR gels can be applied to develop a novel type of permeation media with fluctuating mesh sizes. By controlling the sliding dynamics of the cross-linking points, the rheological and permeation properties of the SR gels can change drastically. The probe diffusion method by DLS is quite useful to evaluate the network fluctuation caused by the sliding motion in SR gels and allows us to control their physical properties based on nanoscale dynamics.

Acknowledgement

This work was supported by ImPACT Program of Council for Science, Technology and Innovation (Cabinet Office, Government of Japan), a Grant-in-Aid for Young Scientists

(B) (No. 15K17905), AIST-UTokyo Advanced Operando-Measurement Technology Open Innovation Laboratory (OPERANDO-OIL) , JST-Mirai Program Grant Number JPMJMI18A2, JST CREST Grant Number JPMJCR1992, and the Materials Education Program for the future leaders in the Research, Industry, and Technology (MERIT). The small-angle X-ray scattering experiments were performed at beamlines BL-6A at the Photon Factory, High Energy Accelerator Research Organization, KEK, with the approval of the Photon Factory Program Advisory Committee (Proposal No. 2015G716).

References

1) Gennes P De, *Physica A*, 271, 231 (1999).

2) Ito K, Kato K, Mayumi K, "*Polyrotaxane and Slide-Ring Materials*", (2015), Royal Society of Chemistry, Cambridge.

3) Takata T, *Polym J*, 38, 1 (2006).

4) Okumura Y, Ito K, *Adv Mater*, 13, 485 (2001).

5) Ito K, *Polym J*, 39, 489 (2007).

6) Liu C, Kadono H, Mayumi K, Kato K, Yokoyam H, Ito K, *ACS Macro Lett*, 6, 1409 (2017).

7) Jiang L, Liu C, Mayum K, Kato K, Yokoyama H, Ito K, *Chem Mater*, 30, 5013 (2018).

8) Liu C, Kadono H, Yokoyama H, Mayumi K, Ito K, *Polymer* 181, 121782 (2019).

9) Katsuno C, Konda A, Urayama K, Takigawa T, Kidowaki M, Ito K, *Adv Mater* 25, 4636 (2013).

10) Shinohara Y, Kayashima K, Okumura Y, Zhao C, Ito K, Amemiya Y, *Macromolecules*, 39, 7386 (2006).

11) Shibayama M, Karino T, Domon Y, Ito K, *J Appl Crystallogr*, 40, 43 (2007).

12) Karino T, Okumura Y, Ito K, Shibayama M, *Macromolecules*, 37, 6177 (2004).

13) Karino T, Okumura Y, Zhao C, Kataoka T, Ito K, Shibayama M, *Macromolecules*, 38, 6161 (2005).

14) Shibayama M, *Macromol Chem Phys*, 199, 1 (1998).

15) Asai H, Nishi K, Hiroi T, Fujii K, Sakai T, Shibayama M, *Polymer*, 54, 1160 (2013).

16) Zhao C, Domon Y, Okumura Y, Okabe S, Shibayama M, Ito K, *J Phys Condens Matter*, 17, S2841 (2005).

17) Mayumi K, Ito K, *Polymer*, 51, 959 (2010).

18) Rose S, Marcellan A, Hourdet D, Creton C, Narita T, *Macromolecules*, 46, 4567 (2013).

19) Kuhn W, *Kolloid-Z*, 68, 2 (1934).

20) Ito K, *Polym J*, 44, 38 (2012).

21) Mayumi K, Tezuka M, Bando A, Ito K, *Soft Matter*, 8, 8179 (2012).

22) Guth E, *J Appl Phys*, 16, 20 (1945).

23) Lin WC, Marcellan A, Hourdet D, Creton C, *Soft Matter*, 7, 6578 (2011).

24) Crichton MA, Bhatia SR, *J Appl Polym Sci*, 93, 490 (2004).

25) Kawasaki Y, Watanabe H. Uneyama T, *Nihon Reoroji Gakkaishi*, 39, 127

(2011).

26) Ohnishi M, Katashima T, Nakahata M, Urakawa O, *Nihon Reoroji Gakkaishi*, 47, 133 (2019)

27) Rubinstein M, Colby RH, "*Polymer Physics*", (2003), Oxford University Press, Oxford.